Microwave Ionization of H Atoms: Breakdown of Classical Dynamics for High Frequencies

E. J. Galvez,[(1),(a)] B. E. Sauer,[(1)] L. Moorman,[(1)] P. M. Koch,[(1)] and D. Richards[(2)]
[(1)]*Physics Department, State University of New York, Stony Brook, New York 11794*
[(2)]*Mathematics Faculty, Open University, Milton Keynes MK7 6AA, United Kingdom*
(Received 18 August 1988)

We report the first measurements of microwave excitation and ionization of excited hydrogen atoms for scaled frequencies $n_0^3\omega$ up to 2.8. Classical 3D calculations which directly model this 36.021-GHz experiment agree quite well for $n_0^3\omega < 1$, agree less well for $1 \leq n_0^3\omega \leq 2$, and do not agree for $n_0^3\omega > 2$. This supports theoretical predictions that as $n_0^3\omega$ rises above 1, quantal ionization threshold fields rise above those for the onset of classical chaos; however, the data continue to reveal local stability near certain rational frequency ratios that recalls classical behavior.

PACS numbers: 05.45.+b, 32.80.Rm, 42.50.Tj

Two Hamiltonian systems have emerged as complementary testing grounds for the study of quantal dynamics in a classically chaotic system, which we take to define the problem of *quantum chaos*.[1,2] Both involve the hydrogen atom. The time-independent problem of excited hydrogen in an intense magnetic field[3] focuses on the properties[4] of its quantal energy spectrum when the underlying classical motion passes from regular to irregular with increasing magnetic field strength.

This Letter concerns the time-dependent problem of the (de-)excitation and ionization[5-8] of excited hydrogen atoms by an intense oscillatory electric field $A(t)F \times \sin(\omega t + \phi)$. $A(t)$ is a slowly varying "envelope" function, F is the electric amplitude, and ϕ is a phase that, so far, experiment has averaged. Useful quantities[9] are the *scaled field* n_0^4F, the ratio of F and the mean unperturbed Coulomb field, and the *scaled frequency* $n_0^3\omega$, the ratio of ω and the unperturbed orbital frequency. We used the fixed frequency $\omega/2\pi = 36.021(2)$ GHz and principal quantum numbers $n_0 = 45$–80 for the first penetration into the region $n_0^2\omega > 1$, stepwise covering the entire range 0.499–2.804.

Large numerical 1D[1,10-13] and 2D[14] calculations, supported by differing[1,10-16] analytical theories, have predicted for $n_0^3\omega$ rising above 1, an increasing stability of the quantal atom over its classical counterpart. Our new results for 3D atoms confirm this predicted quantal effect, showing that when $n_0^3\omega > 2$ measured threshold fields for appreciable flow of population to higher bound states and the continuum rise systematically above those for the onset of classical chaos. However, the effect of local stability near certain rational fraction values of $n_0^3\omega > 1$, previously observed[8] for $n_0^3\omega \lesssim 1$, continues as a prominent feature of our data in this high-frequency, "quantal" domain.

Let us recall previous results[6,8,17-19] for $0.05 \leq n_0^3\omega \leq 1.1$ using the frequencies 7.58, 9.92, and 11.89 GHz and 3D atoms with $n_0 = 32 - 90$: (i) Measured "ionization" and "quench" curves were quite accurately reproduced[8] by classical 3D calculations,[20] but poorer agreement near classical resonances [and see (iii) below] suggested the importance of quantal effects there. Even classical 1D calculations[8,21,22] for the onset of ionization (chaos) explained quite well the $n_0^3\omega$ dependence of the 10% ionization threshold fields. Locally higher threshold fields observed near certain resonances, $n_0^3\omega \simeq 1/p$, $p = 1, 2, \ldots$, were linked to the temporal periodicity of the Hamiltonian. Poincaré "surface-of-section" plots[21,22] in the 1D classical phase space revealed nonlinear resonance trapping regions, or "islands," which have a quantal (1D) analog.[22] That such islands lead to locally stability is well known[23]; here it is theoretically enhanced[22] by the slow field turn on [$A(t)$]. (ii) Quantal 1D calculations[16] also agreed well with 3D experimental 10% ionization threshold fields. (iii) Ionization curves for some low $n_0^3\omega \lesssim 0.2$ values contained "structures"[6,8,17,19] that were not reproduced by classical calculations. They were explained by two different quantal 1D theories[16,17,24] that have recently been linked.[17] (iv) "Classical scaling," i.e., how invariant is n_0^4F as n_0 and ω are varied but $n_0^3\omega$ is kept (nearly) constant, was observed[18] to be reasonably valid for $n_0^3\omega \lesssim 1$ and is further confirmed by some of our present 36.02-GHz results, but the "quantal structures" in (iii) do not scale classically.

The new measurements required refined experimental techniques.[6,8,17-19] Referring to Fig. 1, a 14.6-keV beam of $H(n_0)$ atoms was produced by electron transfer collisions and subsequent laser-double-resonance excitation; neither laser beam entered the microwave cavity,[25] whose electric field was linearly polarized along the

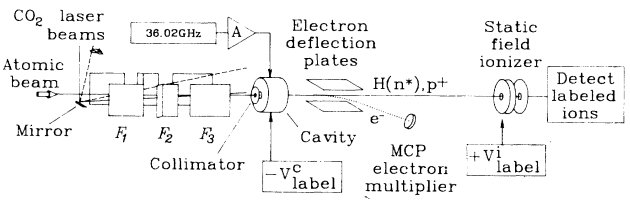

FIG. 1. Schematic view of the experimental arrangement.

beam axis. Previous work[8] showed the distribution of atomic substates entering the cavity to be consistent with a microcanonical ensemble[9,20] with fixed principal action $I_0 = n_0\hbar$. Microwave power was coupled into the cavity through an iris from a waveguide circuit that included model 6913 power sensors ably calibrated specially by Marconi Instruments Ltd. and other components calibrated by us. Electronics both controlled the frequency and repetitively ramped the power to permit signal averaging of experimental signals described below. Using a procedure described in Ref. 26, we converted measured power to absolute microwave electric amplitude to 5% accuracy. In their rest frames each atom saw the spatial variation[25] of the microwave field as a constant [$A(t) > 0.95$] amplitude lasting 334 field oscillations between a turn-on and turn-off [$A(t)$ between 0.05 and 0.95] each lasting 82 oscillations.

Data were taken in two different modes.[8] The "ionization" mode (IM) detected atoms actually ionized plus those excited to $n \geq n_c^i$, a cutoff value of n determined by ionization in static fields after the cavity. Electrons were accelerated *after the cavity* through a potential difference applied to it, $-V_{\text{label}}^{\text{f}} \simeq -6V$; those with initial kinetic energy $(m_e/M_p)14.6$ keV$\simeq 8$ eV that came from fast beam atoms were boosted to about 14 eV and were deflected by $F_e \simeq 0.5$ V/cm. Only electrons "energy labeled" near 14 eV were transmitted through appropriately biased wire meshes into a microchannel-plate electron multiplier. By varying both $V_{\text{label}}^{\text{f}}$ and F_e, we verified complete transmission of signal electrons to the microchannel plate. The computed range $\simeq 0.5$–1 V/cm of the field produced by $V_{\text{label}}^{\text{f}}$ after the cavity set the value of $n_c^i \simeq 160$–190.

The "quench" mode (QM) registered the microwave-induced loss (by ionization and excitation to final states $n \gtrsim n_c^q$) of the proton signal generated in a static field ionizer well downstream of the cavity. Computed and experimentally derived limits on relevant apparatus fields $\simeq 9$–12 V/cm set the value of $n_c^q \simeq 86$–92.

For each mode we varied the microwave power from a value too small to produce a signal to an empirically set large power. The IM and QM curves usually varied from 0% to 100% signal over an enormous dynamic range of power.[27]

Figures 2(a) and 3(a) show, respectively, microwave scaled fields that produced[28] 10% "quenching" [$n_0^4 F_q(10\%)$] or 10% "ionization" [$n_0^4 F_i(10\%)$], with each n_0 value corresponding to a given $n_0^3\omega$. Continuing the effect observed previously,[8,18,19] for $n_0^3\omega < 1.1$, Fig. 2(a) shows locally higher $n_0^4 F_q(10\%)$ thresholds for $n_0^3\omega$ values near rational fractions such as $\frac{1}{1}$, $\frac{4}{3}$, $\frac{2}{1}$, $\frac{5}{2}$, $\frac{8}{3}$, and, perhaps, others. The keen reader wondering why there is no local stability for $n_0^3\omega \simeq \frac{3}{2}$ may be interested to know that the $n_0 = 65$ QM curve contained definite (perhaps even nonmonotonic) "structure" near threshold. We infer that a quantal resonance phenomenon is responsible for this behavior.

Classical 3D calculations[9,20] used a conventional

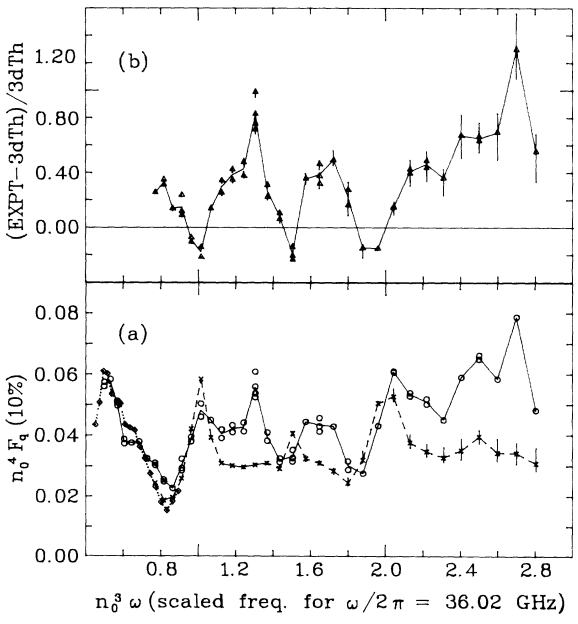

FIG. 2. Curves have been drawn to guide the eye. (a) Scaled 10%-threshold fields for (○) experimental "quench" mode (QM) and (×, ◇) 3D classical calculations vs scaled frequency. (b) △, fractional differences between ○ and × from (a). For vertical line segments in (a) and (b), see text.

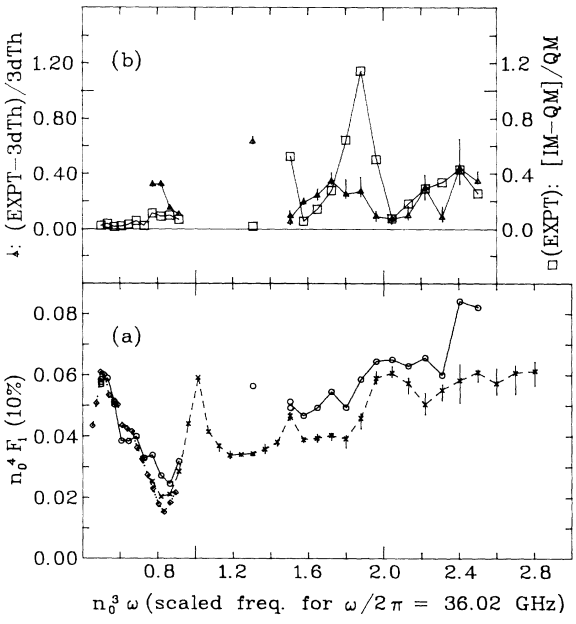

FIG. 3. Curves have been drawn to guide the eye. (a) Same as Fig. 2(a) except ○ are experimental "ionization" mode (IM) results. (b) △, fractional differences between ○ and × from (a); □, fractional differences between IM [Fig. 3(a)] and QM [Fig. 2(a)] 10%-threshold fields.

Monte Carlo method, choosing initial conditions from a stratified sample of a microcanonical ensemble, integrating Hamilton's equations in regularized coordinates[20] to avoid problems with the Coulomb singularity, and using for the "envelope function" $[A(t)]$ a cubic spline fit to the experimental profile.[25] From each set of final orbital parameters, we obtained final Stark actions and used the classical results from Ref. 29 to find the critical static field needed to ionize each orbit (zero for orbits that ionized inside the cavity). This included the effect of static field ionization of atoms excited to above a cutoff n value. To simulate the QM and IM experiments, respectively, and to investigate the sensitivity to the static field, two groups of three fields each—QM (6,8.9,12 V/cm) and IM (0.35,0.53,0.95 V/cm)—were used for analysis. In Figs. 2(a) and 3(a) the top (bottom) [cross] of each vertical line segment shows the classical microwave 10% threshold for the smallest (largest) [middle] of the three field values.[28] [Diamonds are earlier results[20] (from modeling of 9.92-GHz experiments) for which the cutoff n value $\simeq 95$ and the numbers of oscillations (turn-on and turn-off, 50; constant part, 300) were close to those for the present QM simulations.]

Figure 2(b) shows the fractional differences between the QM and classical 10%-threshold fields. The QM data for $n_0^3\omega < 2$ display an intriguing oscillatory behavior in the fractional difference, with five experimental thresholds even lying below classical ones. For $n_0^3\omega > 2$, however, experiment rises systematically above classical theory, at $n_0 = 79$ more than twice as large. These data clearly show a breakdown of classical dynamics for $n_0^3\omega \gtrsim 2$, but the persistence of the undulatory pattern[28] obviously requires further study. Comparisons for other quenching probabilities produce the same general behavior.

For $n_0^3\omega \gtrsim 2$ systematically lower fractional differences [△ in Fig. 3(b)] between IM and classical 10%-threshold fields, compared to corresponding QM data [△ in Fig. 2(b)], suggest that classical dynamics may be less in error for excitation to states way above n_0 (recall that n_c^i is about twice n_c^q) than for excitation to those closer to n_0. The undulatory pattern[28] in Fig. 3(b) is weaker than but matches with that in Fig. 2(b).

We emphasize that this comparison between experiment and classical theory is for a fixed number of field oscillations. (Future experiments will explicitly vary this parameter.) General considerations[1,2] suggest that there is a critical time τ_c depending on F, ω, and n_0 below which classical dynamics is valid. Its effect has been seen in model calculations (e.g., the kicked rotor[1,2]) as well as in numerical 1D[1,10] and 2D[14] studies of microwave excitations and ionization of hydrogen. We do not yet know the behavior of τ_c for 3D hydrogen, but Fig. 4 shows the computed temporal evolution of the classical 3D atom, during and after a 100-oscillation turn-on, for one case, $I_0^3\omega = 2.2195$ (corresponding to $n_0 = 74$ at 36.02 GHz) and $I_0^4F = 0.05$. The orbital parameters of all 256 orbits in the ensemble were sampled regularly; the graph shows the temporal flow to final principal action I_0'. Ionization corresponds to the compensated energy[9,20] $E_c > 0$, and one notices that after the experimental time of 330 field periods (vertical dashed line in Fig. 4), there is scarcely any "true" *classical* ionization.

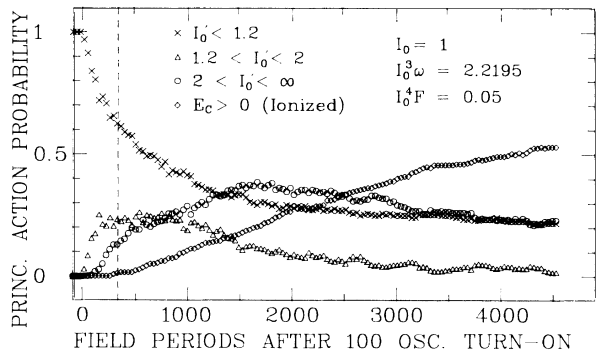

FIG. 4. Computed (3D classical) flow in time from $I_0 = 1$ to final principal action I_0' (binned as shown) and to the continuum ($E_c > 0$).

There is, however, evidence for "true" *experimental* ionization at some $n_0^3\omega$ values. For n_0 values where they were both taken, Fig. 3(b) (□ and right vertical legend) shows fractional differences between IM and QM data. At, e.g., $n_0^3\omega \simeq 1.30, 1.57, 2.04$ nearly equal thresholds (small fractional differences) mean no significant excitation to between the cutoffs n_c^q and n_c^i. Perhaps it has all somehow moved to even higher values $n > n_c^i$, more likely a significant part of it has moved all the way to the continuum. Conversely, at other values of $n_0^3\omega$, particularly at $n_0^3\omega \simeq 1.88$ where IM and QM thresholds differ by more than a factor of 2, there was significant excitation to $n_c^q < n < n_c^i$.

In summary, our results confirm theoretical predictions of quantal excitation-ionization microwave threshold fields rising above classical values when $n_0^3\omega > 2$. Classical 3D calculations that, with no adjustable parameters, modeled 3D experiments so well for $n_0^3\omega \lesssim 1$ have systematically low threshold fields when $n_0^3\omega \gtrsim 2$, but they still retain some of the strong experimental variation with $n_0^3\omega$. The undulatory variation for $n_0^3\omega \gtrsim 1$ has not yet been contained in quantal analytical estimates for "instability borders"[1,10,11-15] variously based on "localization"[1,10,13,14,16] of (diffusive) excitation, uncertainty principle violation,[11] dynamics in a severely truncated "quasiresonant state" basis,[12,13] or quantal versus classical transport through cantori.[15]

We thank the NSF and NATO (travel) for support; G. Casati, B. Chirikov, R. Jensen, J. Leopold, R. MacKay, J. Meiss, and D. Shepelyansky for discussions; K. Altman, L. Belkhir, A. Davis, and D. Mandrus for help; and H. Kirk of BNL for computing facilities.

[a]Present address: Physics Department, Colgate University, Hamilton, NY 13346.

[1]G. Casati *et al.*, Phys. Rep. **154**, 77 (1987).

[2]B. Eckhardt, Phys. Rep. **163**, 205 (1988).

[3]J. Main *et al.*, Phys. Rev. Lett. **57**, 2789 (1986).

[4]D. Delande and J. C. Gay, Phys. Rev. Lett. **59**, 1807 (1987).

[5]J. E. Bayfield and P. M. Koch, Phys. Rev. Lett. **33**, 258 (1974).

[6]P. M. Koch, J. Phys. (Paris), Colloq. **43**, C2-187 (1982).

[7]J. E. Bayfield and L. A. Pinnaduwage, Phys. Rev. Lett. **54**, 313 (1985).

[8]K. A. H. van Leeuwen *et al.*, Phys. Rev. Lett. **55**, 2231 (1985); P. M. Koch, in *Electronic and Atomic Collisions,* edited by H. B. Gilbody *et al.* (Elsevier, Amsterdam, 1988), p. 501; K. A. H. van Leeuwen and P. M. Koch, to be published.

[9]J. G. Leopold and I. C. Percival, Phys. Rev. Lett. **41**, 944 (1978).

[10]G. Casati *et al.*, Phys. Rev. Lett. **53**, 2525 (1984), and Phys. Rev. A **36**, 3501 (1987), and IEEE J. Quantum Electron. **24**, 1420 (1988)—see pp. 1432 and 1435 for the relevance of their theory for "3D" experiments.

[11]J. G. Leopold and D. Richards, J. Phys. B **21**, 2179 (1988).

[12]R. V. Jensen, J. G. Leopold, and D. Richards, J. Phys. B **21**, L527 (1988); D. Richards, J. G. Leopold, and R. V. Jensen, to be published.

[13]R. V. Jensen, S. M. Susskind, and M. M. Sanders, to be published.

[14]G. Casati *et al.*, Phys. Rev. Lett. **59**, 2927 (1987).

[15]R. S. MacKay and J. D. Meiss, Phys. Rev. A **37**, 4702 (1988).

[16]R. Blümel and U. Smilansky, Phys. Rev. Lett. **58**, 2531 (1987), and Z. Phys. D **6**, 83 (1987).

[17]D. Richards *et al.*, to be published.

[18]E. J. Galvez *et al.*, to be published.

[19]L. Moorman *et al.*, Phys. Rev. Lett. **61**, 771 (1988).

[20]O. Rath and D. Richards, to be published.

[21]B. I. Meerson, E. A. Oks, and P. V. Sasorov, J. Phys. B **15**, 3599 (1982); R. V. Jensen, Phys. Rev. A **30**, 386 (1984); J. G. Leopold and D. Richards, J. Phys. B **19**, 1125 (1986); V. Gontis and B. Kaulakys, J. Phys. B **20**, 5051 (1987).

[22]R. V. Jensen, Phys. Scr. **35**, 668 (1987).

[23]B. V. Chirikov, Phys. Rep. **52**, 263 (1979).

[24]D. Richards, J. Phys. B **20**, 2171 (1987).

[25]The field distribution for the 2.007-cm-long, 3.130-cm-diam cylindrical cavity, perturbed from the chosen TM_{040} mode mostly near the 0.258-cm-diam axial hole in each 0.64-cm-thick end cap, was calculated numerically after K. Halbach and R. F. Holsinger, Part. Accel. **7**, 213 (1976). Dropping as a J_0 Bessel function, the microwave electric amplitude at the 0.07-cm radial edge of the collimated atomic beam was 6.9% lower than on the cavity (beam) axis.

[26]B. E. Sauer *et al.*, to be published.

[27]For example, the $n_0=69$ QM signal varied from about 1% quenching at 5.3 V/cm to about 99% at 91 V/cm, a field (power) ratio of about 17 (300). The larger field $n_0^4F\simeq 0.4$ is above the classical static ionization threshold field for *all* of the substates of $n_0=69$, see D. Banks and J. G. Leopold, J. Phys. B **11**, 37 (1978).

[28]A brief discussion of errors: Classical 3D 10%-threshold fields were determined typically to 4%. Apart from the 5% absolute field calibration uncertainty, statistical errors in $n_0^4F_q(10\%)$ and $n_0^4F_i(10\%)$ generally, but nonmonotonically, increased with n_0 and were $\lesssim 5\%$ (6%, once up to 13%) for $n_0^3\omega$ below (above) 2.2. All positive- and negative-going [positive-going] structures in Fig. 2(b) [in Fig. 3(b) (□ and △)] are highly significant with respect to combined experimental and theoretical errors.

[29]Banks and Leopold, Ref. 27.